Cardiac fibroblast-specific p38α MAP kinase promotes cardiac hypertrophy via a paracrine interleukin-6 signalling mechanism

Sumia A. Bageghni PhD[1], Karen E. Hemmings PhD[1], Ngonidzashe Zava BSc[1], Christopher Denton PhD FRCP[2], Karen E. Porter PhD[1], Justin F. X. Ainscough PhD[1], Mark J. Drinkhill PhD[1], Neil A. Turner PhD[1]

[1]Division of Cardiovascular and Diabetes Research, and Multidisciplinary Cardiovascular Research Centre, Leeds Institute of Cardiovascular and Metabolic Medicine, School of Medicine, University of Leeds, Leeds, LS2 9JT, UK;
[2]Centre for Rheumatology, University College London Division of Medicine, Royal Free Campus, Rowland Hill Street, London, NW3 2PF, UK.

Short title: Fibroblast p38α regulates cardiac hypertrophy via IL-6

Corresponding Author: Dr Neil A. Turner, Division of Cardiovascular & Diabetes Research, LIGHT Laboratories, Clarendon Way, University of Leeds, Leeds LS2 9JT, UK. Tel: +44(0)113-3434817. E-mail: n.a.turner@leeds.ac.uk

Word count: 6980

ABSTRACT

Rationale: The p38 family of stress-activated MAP kinases have important functions in cardiac signalling and in cardiomyocyte hypertrophy following myocardial injury or stress. However the specific role of cardiac fibroblast p38α in hypertrophic remodelling of the heart *in vivo* is unknown.

Objective: To elucidate the role of p38α in cardiac fibroblasts in modulating cardiac hypertrophic remodelling.

Methods and Results: A fibroblast-specific tamoxifen-inducible p38α knockout mouse model was developed by crossing Col1a2-Cre-ER(T) mice with floxed p38α (*Mapk14*) mice. Tamoxifen-injected male mice (Cre-negative control or Cre-positive knockout) underwent myocardial injury at 10-12 weeks of age by subcutaneous mini-osmotic pump infusion of the β-adrenergic receptor agonist isoproterenol (ISO) or saline control for 2 weeks. Cardiac function was assessed by Millar conductance PV catheter and heart samples analysed for mRNA and microRNA expression by real-time RT-PCR. ISO infusion in control mice promoted overt cardiac hypertrophy and dysfunction: increased end systolic volume, reduced ejection fraction, increased heart weight/tibia length ratio, upregulation of myocyte hypertrophy markers (ANF, β-MHC) and up-regulation of hypertrophy-associated microRNAs. Fibroblast-specific p38α knockout mice exhibited protection against myocardial injury, with ISO-induced alterations in cardiac function, histology and molecular markers all being attenuated. *In vitro* mechanistic studies revealed a role for p38α-dependent secretion of the cardiomyocyte hypertrophy-inducing factor interleukin-6 (IL-6) from cardiac fibroblasts in response to cardiac damage-associated molecular patterns.

Conclusions: p38α in cardiac fibroblasts plays a key role in driving cardiomyocyte hypertrophy and cardiac dysfunction via a mechanism involving paracrine fibroblast-to-myocyte IL-6 signalling.

Key Words: cardiac fibroblasts • p38 MAP kinase • cardiac hypertrophy • interleukin-6

Non-standard Abbreviations and Acronyms

CO	Cardiac output
DAMPs	Damage-associated molecular patterns
EDP	End diastolic pressure
EDV	End diastolic volume
EF	Ejection fraction
ESV	End systolic volume
ESP	End systolic pressure
Fb-p38α KO	Tamoxifen-inducible fibroblast-specific p38α knockout mouse line
FGF2	Fibroblast growth factor 2
HR	Heart rate
IGF-1	Insulin-like growth factor-1
IL-6	Interleukin-6
ISO	Isoproterenol
LV	Left ventricular
Mapk14	Gene encoding p38α protein
MHC	Myosin heavy chain
PV	Pressure-volume
SV	Stroke volume
TGF-β	Transforming growth factor-β
WGA	Wheat germ agglutinin

INTRODUCTION

The p38 family of stress-activated MAP kinases plays an important role in cardiac signalling and is activated in both acute and chronic cardiac pathologies including myocardial infarction, left ventricular (LV) remodelling, contractile dysfunction, arrhythmia and heart failure.[1-4] A host of pre-clinical studies have demonstrated that p38 MAPK inhibition can reduce the adverse consequences of cardiac injury or stress.[1-4]

There are four known p38 MAPK subtypes (α, β, γ, δ); p38α and p38β share sequence homology and unlike p38γ and p38δ, are inhibited by the pyrindinyl imidazole class of p38 inhibitors (e.g. SB203580). The expression and function of individual p38 subtypes varies in a cell- and tissue-dependent manner; p38α is the most highly expressed subtype in the heart, with lower levels of p38γ and p38δ, and little or no expression of p38β.[5-7] p38α knockout mice are not viable due to an essential role for this subtype in placental development.[8]

Many studies on p38 MAPK in the heart have explored the role of the α and β subtypes.[1-4] *In vitro* experiments involving ectopic over-expression of p38α/β suggested a role for the β rather than the α subtype in stimulating cardiomyocyte hypertrophy.[9,10] However, the relatively low endogenous expression of p38β in human,[5] mouse[6] and rat[7] hearts compared with p38α and other p38 subtypes, may question the physiological importance of these findings. Several studies in a variety of species and cardiac injury models have reported that pharmacological p38α/β inhibition is effective at reducing cardiac hypertrophy.[11] One such study demonstrated that a p38α-selective inhibitor was protective against isoproterenol (ISO)-induced cardiac hypertrophy and dysfunction in rats;[12] suggesting it is p38α rather than p38β that is important in mediating cardiac hypertrophy *in vivo*. However, when p38α has been selectively inhibited in cardiomyocytes *in vivo* (using either cardiomyocyte-specific knockout or dominant negative approaches) there was no apparent benefit on cardiac or cardiomyocyte hypertrophy and some studies reported worsened hypertrophy.[13-16] Similar negative results were obtained with cardiomyocyte-restricted expression of dominant negative p38β.[14] Thus, there is clear discord between pharmacological and cardiomyocyte-specific targeted genetic approaches in ascribing roles to p38α and p38β in cardiac hypertrophy.

A possible unifying explanation for these disparate *in vivo* data relates to cell type specificity. Whilst pharmacological inhibitors and global knockout models affect all cell types, "cardiac-specific" alpha-myosin heavy chain (αMHC)-driven genetic models (knockout or dominant negative) specifically target cardiomyocytes. It has been widely assumed that the inhibitory effects of p38 inhibitors on cardiac hypertrophy are due directly to inhibition of cardiomyocyte p38 activity, with little attention given to other cardiac cell types.

Cardiac fibroblasts are one of the most prevalent non-myocyte cell populations in the heart; accounting for between one-quarter and two-thirds of cardiac cells depending on the species.[17,18] Although traditionally viewed solely in relation to extracellular matrix remodelling, cardiac fibroblasts are now acknowledged as being important nodal regulators of multiple aspects of cardiac function under both physiological and pathophysiological conditions.[19-21] Recent evidence has established a critical role for fibroblasts in inducing cardiomyocyte hypertrophy through paracrine secretion of growth factors and other signalling molecules.[22,23]

To address the role of fibroblast p38α in modulating cardiac hypertrophy *in vivo*, we developed an inducible fibroblast-specific p38α knockout mouse model and investigated cardiac function and molecular changes in a chronic β-adrenergic receptor activation model of cardiac hypertrophy. Our data provide evidence that cardiac fibroblast p38α is integral to ISO-induced cardiac hypertrophy and dysfunction due to a paracrine signalling mechanism involving fibroblast secretion of the cardiomyocyte hypertrophy-inducing factor interleukin-6 (IL-6).

4

METHODS

Animal welfare

All animal procedures were carried out in accordance with the Animal Scientific Procedures Act (UK) 1986 under UK Home Office authorisation following review by the University of Leeds Animal Welfare and Ethical Review Committee. Mice were maintained in GM500 individually ventilated cages (Animal Care Systems) at 21°C, 50-70% humidity, 12/12 h light/dark cycle with Pure-o'Cel paper bedding (Datesand) and *ad libitum* access to water and RM1 diet (Special Diets Services).

Generating an inducible fibroblast-specific p38α knockout mouse model

A tamoxifen-inducible fibroblast-specific p38α knockout mouse line (Fb-p38α KO) was established by crossing C57BL/6 mice expressing fibroblast-specific tamoxifen-inducible Cre recombinase (Col1a2-Cre-ER(T))[24,25] with C57BL/6 mice expressing a modified p38α (*Mapk14*) gene with exons 2-3 flanked by loxP sites[26] (Fig. 1A, Suppl. Fig. 1). The Col1a2-Cre-ER(T) line induces gene deletion in cardiac (and other) fibroblasts without effects on cardiomyocytes, endothelial cells, smooth muscle cells, progenitor cells, pericytes or macrophages.[27,28] Fb-p38α KO mice (i.e. Cre-positive *Mapk14*^{fl/fl}) were compared alongside control littermates (i.e. Cre-negative *Mapk14*^{fl/fl}) for the main experimental protocols. Mice were injected with tamoxifen dissolved in corn oil (100 mg/kg/day i.p. for 5 consecutive days) at 3 weeks of age to induce Cre activity and facilitate loxP-directed deletion.

Genotyping PCR

DNA was extracted from ear notch samples using a phenol:chloroform extraction method after incubation of samples overnight at 37°C in lysis buffer (50 mmol/L EDTA, 10 mmol/L Tris-HCl pH 8.0, 1% (w/v) SDS, 0.5 mg/mL proteinase K). End-point PCR (94°C 3 min, 35 cycles x [94°C 30 s, 62°C 30 s, 72°C 30 s], 72°C 3 min, 4°C hold) was performed with specific primer pairs (see Suppl. Table 1 for details) and agarose gel electrophoresis was used to identify the presence of Cre, floxed *Mapk14* and deletion of *Mapk14* exons 2-3.

Cardiac fibroblast culture

Cardiac fibroblasts were cultured from mouse hearts by collagenase digestion, as described previously.[29] Briefly, hearts were thoroughly washed in phosphate buffered saline and minced prior to digestion with Worthington Type II collagenase (2 mg/mL, 600 IU/mL) at 37°C for 90 min with regular shaking. Cells were pelleted by centrifugation and washed twice in culture medium before seeding into 3 wells of a 6-well tissue culture plate (one each for DNA, RNA and protein analysis) or a 25cm² cell culture flask for subsequent passaging. Non-adherent cells were removed after 30 min and cells incubated with full growth medium (Dulbecco's modified Eagle's medium+10% foetal calf serum). Cells were washed twice with phosphate buffered saline the next day to remove residual non-adherent cells and fresh growth medium added. Primary cultures of cells were analysed for p38α expression 4 days after plating. Passage 1 cells were used for *in vitro* mechanistic studies.

Cardiac cell fractionation

Collagenase-digested hearts were filtered through a 30 μm MACS smart strainer (Miltenyi Biotec) to remove cardiomyocytes. Non-myocytes were separated into two fractions; 'non-fibroblasts' (endothelial cells and leukocytes) and 'fibroblasts' using a cardiac fibroblast magnetic antibody cell separation kit (MACS; Miltenyi Biotec). RNA was extracted from cell fractions and qRT-PCR used to quantify mRNA for cell type-specific marker genes and p38α. Gene expression levels were compared with those obtained from collagenase-digested whole heart.

RNA extraction, cDNA synthesis and real-time RT-PCR

RNA was extracted from cultured/fractionated cells using the Aurum RNA extraction kit (BioRad) or from heart tissue using TRI reagent (Sigma-Aldrich). cDNA was synthesised using

the Promega Reverse Transcription System. Real-time RT-PCR was performed using an ABI-7500 System with gene expression mastermix and specific Taqman primer/probe sets from Applied Biosystems (details in Suppl. Table 2). Data are expressed relative to *Gapdh* housekeeping gene mRNA expression using the $2^{-\Delta CT}$ method.

Western blotting
Western blotting was performed as described previously[30] using Cell Signaling Technology antibodies for p38α (#9228), phospho-p38 (#9211) and phospho-HSP27 (#2401). Horseradish peroxidase-conjugated anti-mouse and anti-rabbit secondary antibodies and ECL detection reagent were from GE Healthcare. Monoclonal β-actin antibody (ab8226; Abcam) was used as a loading control.

Isoproterenol infusion
Mini-osmotic pumps (Alzet 1002) were implanted subcutaneously in isofluorane-anaesthetised mice (control and Fb-p38α KO) as described previously[31] and saline or ISO (30 mg/kg/day) infused for 14 days. Pumps were removed under isofluorane anaesthesia before recovery and analysis of cardiac function 1 week later. Group sizes were: control-saline (n=11), control-ISO (n=9), Fb-p38α KO-saline (n=8) and Fb-p38α KO-ISO (n=11).

Measurement of cardiac function and cardiac weight index
Physiological measurements of cardiac function were obtained at the end of the experimental period by Millar conductance pressure-volume (PV) catheter analysis as described previously.[32] Briefly, mice were anaesthetised with isofluorane and body temperature maintained with a heating pad before inserting a 1.4 F miniature PV catheter (PVR-1045/SPR-839; Millar) into the left ventricle via the right carotid artery and ascending aorta. Data were collected via an MPVS-300 pressure volume system (Millar) and PV loop analysis was performed using Chart 8 Pro software (AD Instruments). 7 animals (18%) did not survive the procedure resulting in final group sizes of: control-saline (n=9), control-ISO (n=8), Fb-p38α KO-saline (n=7) and Fb-p38α KO-ISO (n=8). The investigator performing the PV measurements was blinded to the genotype of the animals.

Hearts were subsequently excised, cleaned, atria removed and ventricles weighed. Tibia were also collected, cleaned and measured. Cardiac weight index was calculated as ventricular weight to tibia length ratio. Ventricles were snap frozen and stored at -80°C for further analysis.

Histology
Cryosections of ventricular tissue (8 μm thickness) were mounted on poly-L-lysine-coated slides and fixed with 4% paraformaldehyde for 20 min. Sections were incubated with rhodamine-labelled wheat germ agglutinin (WGA, 1:1000; Vector Laboratories) for 2 h, washed with phosphate buffered saline, then mounted using VectaShield containing DAPI (Vector Laboratories). Confocal images were captured using a Zeiss LSM700 fluorescence microscope with X40 objective and ZEN 2.1 SP1 software (Zeiss). Cardiomyocyte cross-sectional areas were averaged from 7 or 8 animals per group, with 10 fields of view analysed per animal using Corel PaintShop Pro X8 and Image J (NIH). Measurements were performed in a blinded fashion and by two independent observers.

MicroRNA RT-PCR array
cDNA was synthesised from 4 cardiac RNA samples for each of three groups (control-saline, control-ISO, Fb-p38α KO-ISO) using miScript II Reverse Transcription kit (Qiagen) before performing a miScript miRNA PCR Array (MIMM-113ZA; Qiagen) using the ABI-7500 Real-Time PCR System. This SYBR-Green based array enabled expression levels of 84 cardiovascular-related miRNAs to be analysed. Data are expressed relative to the geometric mean of the 6 normalisation controls included on the array (SNORD61, SNORD68, SNORD72, SNORD95, SNORD96A, RNU6-2) using the $2^{-\Delta CT}$ method.

Preparation of cardiac DAMPs

Murine hearts were excised, cleaned and subjected to freeze/thaw and homogenisation in 2 ml phosphate buffered saline per heart to disrupt tissue and cellular structure. The resultant homogenate was centrifuged to remove debris and the supernatant filter-sterilised before aliquoting for long-term storage at -80°C.

Statistical analysis

Statistical analyses were performed using GraphPad Prism 6 Software (www.graphpad.com). All data are mean values ± SEM. n represents the number of separate animals investigated or the number of separate hearts from which cells were isolated. Data were analysed by Student's t-test or one-way ANOVA with Sidak post hoc test, as appropriate. P<0.05 was considered statistically significant.

RESULTS

Generation of mice with inducible fibroblast-specific deletion of p38α

To investigate the role of cardiac fibroblast p38α in hypertrophic cardiac remodelling, we generated an inducible fibroblast-specific p38α knockout mouse line. This involved crossing mice expressing fibroblast-specific tamoxifen-inducible Cre recombinase (Col1a2-Cre-ER(T))[24,25] with mice expressing a modified p38α gene (*Mapk14*) with exons 2-3 (coding for the ATP-binding site of the kinase domain) flanked by loxP sites[26] (Fig. 1A, Suppl. Fig. 1). Tamoxifen injection at 3 weeks of age induced Cre activity and resultant Cre-lox directed deletion of *Mapk14* exons 2-3 (Fig. 1A). Deletion was confirmed initially by PCR genotyping of ear notches, i.e. dermal fibroblasts (Fig. 1B), and confirmed in cell cultures. Primary cultures of cardiac fibroblasts from hearts of Fb-p38α KO mice had a 50% reduction of *Mapk14* mRNA (Fig. 1C) and p38α protein (Fig. 1D,E) compared with cells from control mice. Knockdown in freshly isolated cardiac cells was investigated by digesting hearts with collagenase before separating non-myocytes into two distinct cell fractions using a magnetic antibody cell separation technique. Endothelial cells (*Pecam1*-positive) were separated into Fraction 1 along with leukocytes, whereas fibroblasts (*Ddr2*, *Pdgfra*, *Col1a1*, *Col1a2*-positive) were separated into Fraction 2 (Fig. 1F). Evaluation of relative *Gapdh* mRNA expression in the two fractions indicated that approximately 64% of non-myocytes were present in Fraction 1 and 32% in Fraction 2, in agreement with recent comprehensive studies on the cellular composition of the murine heart.[33] A 65% reduction in *Mapk14* mRNA levels was observed in the fibroblast-enriched fraction 2 from Fb-p38α KO mice compared with control mice (Fig. 1G). No reduction in *Mapk14* mRNA levels was evident in the endothelial cell/leukocyte-enriched fraction 1 (Fig. 1G), confirming the fibroblast-specific nature of the deletion. The extent of p38α depletion that we observed in isolated fibroblasts (65%) is similar to that reported in previous studies using the Col1a2-Cre-ER(T) approach.[27]

Fibroblast-specific p38α knockout protects against catecholamine-induced cardiac hypertrophy

The effect of fibroblast-specific p38α knockout was investigated in a chronic β-adrenergic receptor activation model of cardiac hypertrophy. Control or Fb-p38α KO mice were injected with tamoxifen at 3 weeks of age, and then at 10-12 weeks of age were implanted with osmotic mini-pumps delivering saline or ISO (30 mg/kg/day) for 14 days (Fig. 2A). Pumps were removed and the animals left for 1 more week before analysing cardiac function by PV catheter recordings (Fig. 2B). In control mice, ISO induced characteristic cardiac dysfunction and dilatation as measured by several haemodynamic indices, including reduced ejection fraction (EF; control=70.6±4.0, ISO=43.7±3.6 %; P<0.001), reduced stroke volume (SV; control=18.0±1.0, ISO=13.0±1.8 μL; P<0.05), reduced cardiac output (CO; control=10509±744, ISO=7476±1028 μL/min; P=0.06) and increased end systolic volume (ESV; control=8.9±1.3, ISO=17.7±1.8 μL; P<0.001) (Fig. 2C). Fb-p38α KO mice exhibited

remarkable protection against ISO-induced cardiac dysfunction. In Fb-p38α KO mice, ISO treatment did not significantly affect EF (ISO=63.9±4.8 %), SV (ISO=17.6±1.4 μL), CO (ISO=10940±1018 μL/min) or ESV (ISO=11.2±2.0 μL) (Fig. 2C).

Cardiac hypertrophy was investigated by measuring cardiac weight index (ventricular weight / tibia length ratio), expression of hypertrophy-associated foetal cardiomyocyte genes and cardiomyocyte cross-sectional area (Fig. 3). In control mice, ISO induced significant increases of 9% in cardiac weight index (Fig. 3A), 4.6-fold in atrial natriuretic factor (*Nppa*) mRNA expression, 8.6-fold in β-MHC (*Myh7*) mRNA expression (Fig. 3B) and 43% in cardiomyocyte cross-sectional area (Fig. 3C,D). Strikingly, Fb-p38α KO mice showed very little evidence of ISO-induced cardiac hypertrophy measured by any of these methods (Fig. 3A-D). Investigation of fibrotic markers revealed no overt effect of ISO on collagen (*Col1a1* or *Col3a1*) mRNA expression in control hearts 3 weeks after initiation of ISO infusion and there were no differences in collagen expression between control mice and Fb-p38α KO mice (Fig. 3B).

A focused miRNA array was employed to investigate the effect of ISO on selected cardiovascular miRNAs and the influence of fibroblast-specific p38α knockout (Fig. 4). RNA samples prepared from hearts of saline-infused control mice were compared with those of ISO-infused control mice and ISO-infused Fb-p38α KO mice (4 hearts per group) and expression levels of 84 cardiovascular miRNAs evaluated (see Suppl. Table 3 for full data set). The 10 most highly expressed miRNAs in control hearts from saline-infused animals included miR-1a, miR-126a, miR-24 and multiple members of the miR-23, miR-26 and miR-30 families (Fig. 4A). 12 of the 84 miRNAs studied were reproducibly increased in hypertrophic hearts from ISO-infused mice compared with hearts from saline-infused mice (miR-21a, 24, 27a/b, 29a/c, 140, 199a, 208a/b, 214 and 224), and two miRNAs were decreased in ISO hearts compared with saline hearts (miR-30d and 150) (Fig. 4B). Fibroblast-specific p38α knockout opposed the effects of ISO on some of these miRNAs; namely miR-208b, 21a, 214, 224 and 30d (Fig. 4C). P38α knockout also induced miR-328 expression, although it was not modulated by ISO; suggesting negative regulation of this miRNA by fibroblast p38α (Fig. 4C).

Cardiac fibroblast p38α is required for damage-induced secretion of the cardiomyocyte hypertrophy-inducing factor IL-6

Cardiac fibroblasts have been shown to play a critical role in stimulating cardiomyocyte hypertrophy through paracrine secretion of hypertrophic growth factors, including fibroblast growth factor 2 (FGF2), insulin-like growth factor-1 (IGF-1) and transforming growth factor-β (TGF-β).[22,23] We surmised that IL-6 may also play a similar role. Our hypothesis was that cardiac fibroblast p38α could be important for secretion of such cardiomyocyte hypertrophy-inducing factors in our model and that this would explain the ability of cardiac fibroblast p38α deletion to improve cardiac hypertrophy after ISO infusion.

Firstly we investigated whether ISO could directly activate p38 MAPK in cultured cardiac fibroblasts and then whether it could induce myocyte hypertrophy-inducing factors (FGF-2, IGF-1, TGF-β1 and IL-6) in a p38α-dependent manner. Although ISO directly activated fibroblast p38α (Fig. 5A), it was unable to stimulate expression of any of the hypertrophy-inducing genes tested (Fig. 5B).

We next investigated whether ISO could be modulating fibroblast function indirectly by inducing cardiac damage, resulting in release of damage-associated molecular patterns (DAMPs) and fibroblast activation.[20] To mimic this *in vitro*, we prepared cardiac DAMPs by freeze-thawing and homogenising mouse heart tissue. This cardiac DAMPs preparation activated p38α when added to cultured cardiac fibroblasts (Fig. 5A). Cardiac DAMPs did not modulate *Fgf2* mRNA levels, but strongly stimulated *Il6* mRNA expression by >10-fold and increased *Tgfb1* mRNA levels by 50% after 6 h (Fig. 5B). The DAMPs preparation had the opposite effect on *Igf1* mRNA levels, decreasing them by 50% (Fig. 5B). Further investigation into the time course of these effects revealed that the increase in *Il6* and *Tgfb1* mRNA expression returned to basal levels within 24 h, whereas the reduction in *Igf1* levels was maintained for at least 48 h (Fig. 6A). Despite the relatively transient nature of *Il6* mRNA

expression, ELISA analysis of conditioned medium confirmed a sizeable elevation of IL-6 protein secretion in response to cardiac DAMPs, with peak levels of >10 ng/mL maintained for 24-48 h after the initial stimulus (Suppl. Fig. 2). The p38 MAPK inhibitor SB203580 (Merck) was used to evaluate the importance of p38α in mediating DAMPs-induced changes in hypertrophic gene expression. SB203580 prevented p38 MAPK downstream signalling as expected (Fig. 6B) and significantly reduced DAMPs-induced *Il6* mRNA expression and protein secretion (Fig. 6C, 6D). In contrast, the p38 inhibitor had no effect on DAMPs-induced expression of *Tgfb1* or *Igf1* mRNA (Fig. 6C). Together these data indicate that cardiac DAMPs can stimulate IL-6 transcription and protein secretion in a p38α-dependent manner; a mechanism that likely explains our *in vivo* observations.

DISCUSSION

Our study demonstrated that fibroblast-specific knockout of p38α negates the deleterious effects of chronic β-adrenergic receptor stimulation on cardiac hypertrophy and function. Specifically, our *in vivo* experiments revealed that fibroblast-specific p38α knockout prevented the ability of chronic ISO infusion to reduce EF, increase ESV, increase ventricular weight/tibia length ratio, upregulate myocyte hypertrophy markers (atrial natriuretic factor, β-MHC), upregulate pro-hypertrophic miRNAs and downregulate anti-hypertrophic miRNAs. Our supporting *in vitro* experiments indicated a key role for p38α in mediating DAMPs-induced secretion of the cardiomyocyte hypertrophy-inducing factor IL-6 from cardiac fibroblasts. Our study therefore reveals that cardiac fibroblast p38α is important for regulating cardiomyocyte hypertrophy through paracrine fibroblast-to-myocyte signalling involving IL-6 secretion (Fig. 6E).

Despite nearly two decades of study, the precise individual roles of p38α and p38β in modulating cardiomyocyte hypertrophy remain unclear, with seemingly contradictory outcomes reported.[2,3,11] Results from *in vitro* ectopic over-expression studies of individual p38 subtypes in cardiomyocytes are at odds with cardiomyocyte-targeted *in vivo* genetic inhibition studies, yet pharmacological p38α inhibition appears effective at reducing cardiac hypertrophy. Our data offer a unifying explanation by uncovering a role for cardiac fibroblast p38α in modulating cardiomyocyte hypertrophy *in vivo*.

Many stimuli that cause LV hypertrophy (e.g. catecholamines, Ang II, pressure overload) are direct inducers of cardiomyocyte cellular hypertrophy *in vitro*, and this has been assumed to underlie their hypertrophic action on the heart. However, this concept has been challenged by several recent studies showing that fibroblasts act as primary integrators of hypertrophic stimuli in the intact heart.[22,23,34] A number of paracrine signalling molecules have been identified through which fibroblasts can modulate cardiomyocyte hypertrophy, including FGF2, IGF-1 and TGF-β. Additionally, IL-6 may act in this manner as this cytokine is actively secreted from cardiac fibroblasts in response to β-adrenergic receptor stimulation or Ang II,[19] is able to directly induce cardiomyocyte hypertrophy[35] and IL-6 knockout mice are protected against LV hypertrophy in response to noradrenaline, Ang II or pressure overload.[35-37]

The miRNA microarray identified several highly expressed miRNAs in control murine heart tissue, with miR-1, 126a and 30c being the most abundant. Twelve of the 84 miRNAs studied were reproducibly increased, and two were decreased, in hypertrophic hearts from ISO-infused mice compared with hearts from saline-infused mice. Many of these miRNAs have been shown to be modulated similarly in other reports on mouse and rat models of cardiac hypertrophy.[38-42] We identified five miRNAs that were significantly regulated by ISO in control mice but not in Fb-p38α KO mice (miR-208b, 21a, 214, 224 and 30d), suggesting relevance to the cardioprotective effect of fibroblast-specific p38α knockout. MiR-208b lies within an intron of the β-MHC gene so its increase would be expected given the increase in β-MHC (*Myh7*) mRNA expression in ISO hearts. Interestingly, two of the other miRNAs (miR-21a and miR-214) have been shown to positively regulate IL-6 secretion in macrophages and fibroblast-like ligamentum flavum cells.[43,44] These microRNAs may play similar roles in cardiac fibroblasts, contributing to the paracrine IL-6 hypertrophic effect we discovered. We identified

just one miRNA (miR-328) that was elevated in ISO-infused p38 KO hearts compared with ISO-infused control hearts, suggesting negative regulation by fibroblast p38α. Indeed, miR-328 has been shown to be negatively regulated by p38 MAPK in human osteosarcoma cells.[45]

Whilst our study was being finalised, several new reports emerged that also support a critical role for cardiac fibroblast p38α in modulating cardiac remodelling. Firstly, a non-biased transcriptomic approach identified cardiac fibroblast ATF3 as being cardioprotective in HF models; and fibroblast p38 MAPK was identified as the downstream molecule responsible for profibrotic and hypertrophic effects in fibroblast-specific ATF3 KO mice (Col1a2-Cre-ER(T) model).[46] Secondly, global knockdown of MK5 (a p38 substrate localised to cardiac fibroblasts but not myocytes) was associated with the attenuation of both hypertrophy and cardiac dysfunction in response to chronic pressure overload.[47] Thirdly, it was reported that inducible fibroblast-selective knockdown of p38α (using *Tcf21*- and *Postn*-directed Cre KO mouse models) could reduce myofibroblast differentiation and fibrosis following ischemic injury or chronic neurohumoral stimulation.[48] Although focused on fibrosis, this latter study also noted that fibroblast-selective p38α KO reduced cardiac hypertrophy induced by Ang II and phenylephrine infusion.[48] Our study defines a clear hypertrophic role for cardiac fibroblast p38α and identifies IL-6 as a p38α-induced paracrine factor capable of stimulating cardiomyocyte hypertrophy in this setting. Thus, strong evidence is accumulating that p38α in cardiac fibroblasts acts as a central mediator of cardiac hypertrophy and fibrosis in a variety of pathological scenarios, making it an attractive target for therapeutic intervention.

In conclusion, our study reveals an important role for p38α, specifically in cardiac fibroblasts, in stimulating cardiac hypertrophy after chronic β-adrenergic stimulation via an IL-6 dependent mechanism. These findings help to explain the disparity between the effects of pharmacological p38 inhibitors and cardiomyocyte-specific knockout/inhibition models for inhibiting cardiac hypertrophy *in vivo*. They also further our understanding of the key role that cardiac fibroblasts play in regulating cardiac hypertrophy and remodelling through paracrine signalling, and identify the cardiac fibroblast p38α / IL-6 axis as a potential therapeutic target in this setting.

Disclosures
None.

REFERENCES

1. Turner NA. Therapeutic regulation of cardiac fibroblast function: targeting stress-activated protein kinase pathways. *Fut Cardiol.* 2011;7:673-691.

2. Yokota T, Wang Y. p38 MAP kinases in the heart. *Gene.* 2016;575:369-376.

3. Marber MS, Rose B, Wang Y. The p38 mitogen-activated protein kinase pathway-A potential target for intervention in infarction, hypertrophy, and heart failure. *J Mol Cell Cardiol.* 2011;51:485-490.

4. Arabacilar P, Marber M. The case for inhibiting p38 mitogen-activated protein kinase in heart failure. *Front Pharmacol.* 2015;6:102.

5. Lemke LE, Bloem LJ, Fouts R, Esterman M, Sandusky G, Vlahos CJ. Decreased p38 MAPK activity in end-stage failing human myocardium: p38 MAPK α is the predominant isoform expressed in human heart. *J Mol Cell Cardiol*. 2001;33:1527-1540.

6. Dingar D, Merlen C, Grandy S, Gillis MA, Villeneuve LR, Mamarbachi AM, Fiset C, Allen BG. Effect of pressure overload-induced hypertrophy on the expression and localization of p38 MAP kinase isoforms in the mouse heart. *Cell Signal*. 2010;22:1634-1644.

7. Rakhit RD, Kabir AN, Mockridge JW, Saurin A, Marber MS. Role of G proteins and modulation of p38 MAPK activation in the protection by nitric oxide against ischemia-reoxygenation injury. *Biochem Biophys Res Commun*. 2001;286:995-1002.

8. Adams RH, Porras A, Alonso G, Jones M, Vintersten K, Panelli S, Valladares A, Perez L, Klein R, Nebreda AR. Essential role of p38α MAP kinase in placental but not embryonic cardiovascular development. *Mol Cell*. 2000;6:109-116.

9. Wang Y, Huang S, Sah VP, Ross J, Jr., Brown JH, Han J, Chien KR. Cardiac muscle cell hypertrophy and apoptosis induced by distinct members of the p38 mitogen-activated protein kinase family. *J Biol Chem*. 1998;273:2161-2168.

10. Koivisto E, Kaikkonen L, Tokola H, Pikkarainen S, Aro J, Pennanen H, Karvonen T, Rysa J, Kerkela R, Ruskoaho H. Distinct regulation of B-type natriuretic peptide transcription by p38 MAPK isoforms. *Mol Cell Endocrinol*. 2011;338:18-27.

11. Martin ED, Bassi R, Marber MS. p38 MAPK in cardioprotection - are we there yet? *Br J Pharmacol*. 2015;172:2101-2113.

12. Li Z, Tran TT, Ma JY, O'Young G, Kapoun AM, Chakravarty S, Dugar S, Schreiner G, Protter AA. p38 alpha mitogen-activated protein kinase inhibition improves cardiac function and reduces myocardial damage in isoproterenol-induced acute myocardial injury in rats. *J Cardiovasc Pharmacol*. 2004;44:486-492.

13. Nishida K, Yamaguchi O, Hirotani S, Hikoso S, Higuchi Y, Watanabe T, Takeda T, Osuka S, Morita T, Kondoh G, Uno Y, Kashiwase K, Taniike M, Nakai A, Matsumura Y, Miyazaki J, Sudo T, Hongo K, Kusakari Y, Kurihara S, Chien KR, Takeda J, Hori M, Otsu K. p38α mitogen-activated protein kinase plays a critical role in cardiomyocyte survival but not in cardiac hypertrophic growth in response to pressure overload. *Mol Cell Biol*. 2004;24:10611-10620.

14. Zhang S, Weinheimer C, Courtois M, Kovacs A, Zhang CE, Cheng AM, Wang Y, Muslin AJ. The role of the Grb2-p38 MAPK signaling pathway in cardiac hypertrophy and fibrosis. *J Clin Invest*. 2003;111:833-841.

15. Sari FR, Widyantoro B, Thandavarayan RA, Harima M, Lakshmanan AP, Zhang S, Muslin AJ, Suzuki K, Kodama M, Watanabe K. Attenuation of CHOP-mediated myocardial apoptosis in pressure-overloaded dominant negative p38α mitogen-activated protein kinase mice. *Cell Physiol Biochem*. 2011;27:487-496.

16. Braz JC, Bueno OF, Liang Q, Wilkins BJ, Dai YS, Parsons S, Braunwart J, Glascock BJ, Klevitsky R, Kimball TF, Hewett TE, Molkentin JD. Targeted inhibition of p38 MAPK promotes hypertrophic cardiomyopathy through upregulation of calcineurin-NFAT signaling. *J Clin Invest*. 2003;111:1475-1486.

17. Jugdutt BI. Ventricular remodeling after infarction and the extracellular collagen matrix: when is enough enough? *Circulation*. 2003;108:1395-1403.

18. Banerjee I, Fuseler JW, Price RL, Borg TK, Baudino TA. Determination of cell types and numbers during cardiac development in the neonatal and adult rat and mouse. *Am J Physiol Heart Circ Physiol*. 2007;293:H1883-H1891.

19. Porter KE, Turner NA. Cardiac fibroblasts: at the heart of myocardial remodeling. *Pharmacol Ther*. 2009;123:255-278.

20. Turner NA. Inflammatory and fibrotic responses of cardiac fibroblasts to myocardial damage associated molecular patterns (DAMPs). *J Mol Cell Cardiol*. 2016;94:189-200.

21. Dostal D, Glaser S, Baudino TA. Cardiac fibroblast physiology and pathology. *Compr Physiol*. 2015;5:887-909.

22. Fujiu K, Nagai R. Fibroblast-mediated pathways in cardiac hypertrophy. *J Mol Cell Cardiol*. 2014;70:64-73.

23. Kamo T, Akazawa H, Komuro I. Cardiac nonmyocytes in the hub of cardiac hypertrophy. *Circ Res*. 2015;117:89-98.

24. Zheng B, Zhang Z, Black CM, de Crombrugghe B, Denton CP. Ligand-dependent genetic recombination in fibroblasts : a potentially powerful technique for investigating gene function in fibrosis. *Am J Pathol*. 2002;160:1609-1617.

25. Denton CP, Khan K, Hoyles RK, Shiwen X, Leoni P, Chen Y, Eastwood M, Abraham DJ. Inducible lineage-specific deletion of TβRII in fibroblasts defines a pivotal regulatory role during adult skin wound healing. *J Invest Dermatol*. 2009;129:194-204.

26. Heinrichsdorff J, Luedde T, Perdiguero E, Nebreda AR, Pasparakis M. p38α MAPK inhibits JNK activation and collaborates with IκB kinase 2 to prevent endotoxin-induced liver failure. *EMBO Rep*. 2008;9:1048-1054.

27. Lal H, Ahmad F, Zhou J, Yu JE, Vagnozzi RJ, Guo Y, Yu D, Tsai EJ, Woodgett J, Gao E, Force T. Cardiac fibroblast glycogen synthase kinase-3β regulates ventricular remodeling and dysfunction in ischemic heart. *Circulation*. 2014;130:419-430.

28. Ubil E, Duan J, Pillai IC, Rosa-Garrido M, Wu Y, Bargiacchi F, Lu Y, Stanbouly S, Huang J, Rojas M, Vondriska TM, Stefani E, Deb A. Mesenchymal-endothelial transition contributes to cardiac neovascularization. *Nature*. 2014;514:585-590.

29. Mylonas KJ, Turner NA, Bageghni SA, Kenyon CJ, White CI, McGregor K, Kimmitt RA, Sulston R, Kelly V, Walker BR, Porter KE, Chapman KE, Gray GA. 11β-HSD1 suppresses cardiac fibroblast CXCL2, CXCL5 and neutrophil recruitment to the heart post MI. *J Endocrinol*. 2017;233:315-327.

30. Turner NA, Ball SG, Balmforth AJ. The mechanism of angiotensin II-induced extracellular signal-regulated kinase-1/2 activation is independent of angiotensin AT$_{1A}$ receptor internalisation. *Cell Signal*. 2001;13:269-277.

31. Ainscough JF, Drinkhill MJ, Sedo A, Turner NA, Brooke DA, Balmforth AJ, Ball SG. Angiotensin II type-1 receptor activation in the adult heart causes blood pressure-independent hypertrophy and cardiac dysfunction. *Cardiovasc Res*. 2009;81:592-600.

32. Frentzou GA, Drinkhill MJ, Turner NA, Ball SG, Ainscough JF. A state of reversible compensated ventricular dysfunction precedes pathological remodelling in response to cardiomyocyte-specific activity of angiotensin II type-1 receptor in mice. *Dis Model Mech*. 2015;8:783-794.

33. Pinto AR, Ilinykh A, Ivey MJ, Kuwabara JT, D'Antoni ML, Debuque R, Chandran A, Wang L, Arora K, Rosenthal NA, Tallquist MD. Revisiting cardiac cellular composition. *Circ Res*. 2016;118:400-409.

34. Pellieux C, Foletti A, Peduto G, Aubert JF, Nussberger J, Beermann F, Brunner HR, Pedrazzini T. Dilated cardiomyopathy and impaired cardiac hypertrophic response to angiotensin II in mice lacking FGF-2. *J Clin Invest*. 2001;108:1843-1851.

35. Zhao L, Cheng G, Jin R, Afzal MR, Samanta A, Xuan YT, Girgis M, Elias HK, Zhu Y, Davani A, Yang Y, Chen X, Ye S, Wang OL, Chen L, Hauptman J, Vincent RJ, Dawn B. Deletion of interleukin-6 attenuates pressure overload-induced left ventricular hypertrophy and dysfunction. *Circ Res*. 2016;118:1918-1929.

36. Meier H, Bullinger J, Marx G, Deten A, Horn LC, Rassler B, Zimmer HG, Briest W. Crucial role of interleukin-6 in the development of norepinephrine-induced left ventricular remodeling in mice. *Cell Physiol Biochem*. 2009;23:327-334.

37. Coles B, Fielding CA, Rose-John S, Scheller J, Jones SA, O'Donnell VB. Classic interleukin-6 receptor signaling and interleukin-6 trans-signaling differentially control angiotensin II-dependent hypertension, cardiac signal transducer and activator of transcription-3 activation, and vascular hypertrophy in vivo. *Am J Pathol*. 2007;171:315-325.

38. van Rooij E, Sutherland LB, Liu N, Williams AH, McAnally J, Gerard RD, Richardson JA, Olson EN. A signature pattern of stress-responsive microRNAs that can evoke cardiac hypertrophy and heart failure. *Proc Natl Acad Sci U S A*. 2006;103:18255-18260.

39. Cheng Y, Ji R, Yue J, Yang J, Liu X, Chen H, Dean DB, Zhang C. MicroRNAs are aberrantly expressed in hypertrophic heart: do they play a role in cardiac hypertrophy? *Am J Pathol*. 2007;170:1831-1840.

40. Sayed D, Hong C, Chen IY, Lypowy J, Abdellatif M. MicroRNAs play an essential role in the development of cardiac hypertrophy. *Circ Res*. 2007;100:416-424.

41. Diao X, Shen E, Wang X, Hu B. Differentially expressed microRNAs and their target genes in the hearts of streptozotocin-induced diabetic mice. *Mol Med Rep*. 2011;4:633-640.

42. Hou Y, Sun Y, Shan H, Li X, Zhang M, Zhou X, Xing S, Sun H, Chu W, Qiao G, Lu Y. β-adrenoceptor regulates miRNA expression in rat heart. *Med Sci Monit*. 2012;18:BR309-BR314.

43. Sun C, Tian J, Liu X, Guan G. MiR-21 promotes fibrosis and hypertrophy of ligamentum flavum in lumbar spinal canal stenosis by activating IL-6 expression. *Biochem Biophys Res Commun*. 2017;490:1106-1111.

44. Zhao L, Liu YW, Yang T, Gan L, Yang N, Dai SS, He F. The mutual regulation between miR-214 and A2AR signaling plays an important role in inflammatory response. *Cell Signal*. 2015;27:2026-2034.

45. Yang SF, Lee WJ, Tan P, Tang CH, Hsiao M, Hsieh FK, Chien MH. Upregulation of miR-328 and inhibition of CREB-DNA-binding activity are critical for resveratrol-mediated suppression of matrix metalloproteinase-2 and subsequent metastatic ability in human osteosarcomas. *Oncotarget*. 2015;6:2736-2753.

46. Li Y, Li Z, Zhang C, Li P, Wu Y, Wang C, Lau WB, Ma XL, Du J. Cardiac fibroblast-specific activating transcription factor 3 protects against heart failure by suppressing MAP2K3-p38 signaling. *Circulation*. 2017;135:2041-2057.

47. Nawaito SA, Dingar D, Sahadevan P, Hussein B, Sahmi F, Shi Y, Gillis MA, Gaestel M, Tardif JC, Allen BG. MK5 haplodeficiency attenuates hypertrophy and preserves diastolic function during remodeling induced by chronic pressure overload in the mouse heart. *Am J Physiol Heart Circ Physiol*. 2017;313:H46-H58.

48. Molkentin JD, Bugg D, Ghearing N, Dorn LE, Kim P, Sargent MA, Gunaje J, Otsu K, Davis JM. Fibroblast-specific genetic manipulation of p38 MAPK in vivo reveals its central regulatory role in fibrosis. *Circulation*. 2017;136:549-561.

Figure 1. Inducible fibroblast-specific deletion of p38α in mouse heart. **(A)** Schematic diagram of deletion strategy combining Col1a2-Cre-ER(T) mice with floxed *Mapk14* mice. Deletion of exons 2-3 occurs following tamoxifen injection which activates Cre-ER(T). Red arrowheads denote position of genotyping primers X, Y and Z (see Suppl. Table 1). **(B)** Genotyping PCR showing effective exon 2/3 deletion in ear notch samples from tamoxifen-injected experimental Cre-positive Mapk14$^{fl/fl}$ mice (E1-2) compared with control Cre-negative Mapk14$^{fl/fl}$ mice (C1-3). Upper panel: Cre primers (Cre = 408 bp). Lower panel: *Mapk14* exon 2/3 floxed/deletion primers. Deletion (Z+Y) = 411 bp, floxed (X+Y) = 188 bp. M=100 bp ladder. **(C)** Real-time RT-PCR analysis of *Mapk14* mRNA levels in primary cultures of cardiac fibroblasts from control Cre-negative *Mapk14*$^{fl/fl}$ mice (n=6) and Cre-positive *Mapk14*$^{fl/fl}$ knockout (KO) mice (n=8) following tamoxifen injection. *P<0.05. **(D)** Immunoblot analysis of p38α protein in primary cultures of cardiac fibroblasts from control Cre-positive *Mapk14*$^{wt/wt}$ (C), heterozygous Cre-positive *Mapk14*$^{wt/fl}$ (Het) and experimental Cre-positive *Mapk14*$^{fl/fl}$ mice (E1-4) following tamoxifen injection. β-actin loading control. **(E)** Densitometric analysis of p38α protein expression relative to β-actin in control, heterozygous (Het) and experimental (KO) cells. **(F)** Characterisation of non-myocyte isolated cell fractions from collagenase-digested mouse hearts (n=7). Fr1 = endothelial cells and leukocytes; Fr2 = cardiac fibroblasts. Bar charts show qRT-PCR data for mRNA levels of cell type-specific marker genes. Cardiomyocyte marker: *Myh6*. Endothelial marker: *Pecam1*. Fibroblast markers: *Ddr2*, *Pdgfra*, *Col1a1* and *Col1a2*. All data normalised to *Gapdh* mRNA levels and expressed relative to whole heart. **(G)** Real-time RT-PCR analysis of *Mapk14* mRNA levels in isolated cell fractions from hearts of control Cre-negative *Mapk14*$^{fl/fl}$ mice (n=3) and experimental Cre-positive *Mapk14*$^{fl/fl}$ knockout (KO) mice (n=4) following tamoxifen injection. Fr1 = endothelial cells and leukocytes; Fr2 = fibroblasts. **P<0.01, ^{NS} not significant.

Figure 2. Effect of fibroblast-specific p38α knockout on isoproterenol-induced cardiac dysfunction. **(A)** Timeline for chronic β-adrenergic receptor activation model of cardiac hypertrophy. **(B)** Individual representative PV loops obtained from control and fibroblast-specific p38α KO mice following infusion with either saline (control, blue) or isoproterenol (ISO, red). **(C)** PV conductance catheter data. Individual data and mean ± SEM are shown. Group sizes: control saline (n=9), control ISO (n=8), KO saline (n=7), KO ISO (n=8). ANOVA with Sidak post-hoc test: ***P<0.001, *P<0.05, ^{NS} not significant.

Figure 3. Effect of fibroblast-specific p38α knockout on isoproterenol-induced cardiac hypertrophy. Control or Fb-p38α KO mice were injected with tamoxifen and mini-osmotic pumps implanted for delivery of saline or ISO as in Fig. 2A. Pumps were removed and heart tissue collected 1 week later. All data are mean ± SEM. ANOVA with Sidak post-hoc test: ***P<0.001, *P<0.05, ^{NS} not significant. **(A)** Ventricular weight/tibia length ratio (cardiac weight index) from animals used in PV analysis. Group sizes: control saline (n=9), control ISO (n=8), KO saline (n=7), KO ISO (n=8). **(B)** Real-time RT-PCR analysis of mRNA levels for cardiomyocyte hypertrophy markers atrial natriuretic factor (*Nppa*) and β-myosin heavy chain (*Myh7*) and fibrosis markers *Col1a1* and *Col3a1*. Group sizes: control saline (n=11), control ISO (n=9), KO saline (n=8), KO ISO (n=11). **(C)** Representative images of wheat germ agglutinin (WGA)-labelled heart sections used to determine myocyte cross-sectional area. Scale bar = 20 μm. **(D)** Mean cardiomyocyte size (cross-sectional area) determined from WGA-stained images. Group sizes: control saline (n=8), control ISO (n=7), KO ISO (n=8).

Figure 4. Effect of fibroblast-specific p38α knockout on isoproterenol-induced miRNA expression. Control or Fb-p38α KO mice were injected with tamoxifen and infused with saline or ISO as described in Fig. 2A and Fig. 3 legends. Heart tissue was collected 1 week after removal of mini-osmotic pumps and expression levels of 84 cardiovascular miRNAs determined using a real-time RT-PCR array. Group sizes: n=4. See Suppl. Table 3 for full data

set. **(A)** List of the 22 most highly expressed miRNAs in control hearts from saline-infused mice. Data are mean expression levels ($2^{-\Delta CT}$) relative to array normalisation controls. **(B)** MiRNAs increased or decreased following ISO infusion. **P<0.01, *P<0.05 for effect of ISO (unpaired t-test). **(C)** MiRNAs modulated by fibroblast-specific p38α knockout. ANOVA with Sidak post-hoc test: ***P<0.001, **P<0.01, *P<0.05, [NS] not significant compared with control saline group. [#]P<0.05 compared with control ISO group. Data expressed relative to array normalisation controls.

Figure 5. Effects of isoproterenol and cardiac DAMPs on p38α activation and expression of hypertrophy-inducing factors in cultured cardiac fibroblasts. **(A)** Western blotting of phosphorylated (activated) p38α and total p38α expression showing time course of response to 5 μmol/L ISO, concentration response to 0.1-10 μmol/L ISO after 15 min and time course of response to cardiac DAMPs. Blots representative of 3 separate experiments. **(B)** Real-time RT-PCR data showing effect of ISO (5 μmol/L, 6 h, n=8) or cardiac DAMPs (6 h, n=12) on mRNA expression of *Fgf2*, *Il6*, *Tgfb1* and *Igf1*. Data expressed as % *Gapdh* mRNA levels. ***P<0.001, **P<0.01 (paired ratio t-test).

Figure 6. Role of p38α in DAMPs-modulated expression of hypertrophy-inducing genes in cardiac fibroblasts. **(A)** Real-time RT-PCR showing time course of effect of DAMPs on expression of *Il6*, *Tgfb1* and *Igf1*. **P<0.01, *P<0.05 (n=3). **(B)** Western blot showing DAMPs-induced phosphorylation of HSP27 and p38α after 20 min and inhibition by 10 μmol/L SB203580. Total p38α expression included as loading control. Blots representative of 3 separate experiments. **(C)** Real-time RT-PCR data showing effect of 10 μmol/L SB203580 or DMSO vehicle control on DAMPs-induced expression of hypertrophy-inducing genes after 6 h (n=9). ANOVA with Sidak post-hoc test: ***P<0.001, **P<0.01, *P<0.05, [NS] not significant. Data normalised to *Gapdh* mRNA levels and expressed relative to control. **(D)** ELISA showing effect of 10 μmol/L SB203580 or DMSO vehicle control on DAMPs-induced IL-6 secretion after 6 h (n=9). ANOVA with Sidak post-hoc test: *P<0.05, [NS] not significant. **(E)** Schematic depicting role of fibroblast p38α in modulating cardiomyocyte hypertrophy. DAMPs = damage-associated molecular patterns; IL-6 = interleukin-6.

SUPPLEMENTAL MATERIAL LEGENDS

Supplemental Figure 1. Breeding strategy for generating Col1a2-Cre-ER(T) positive (experimental) and Col1a2-Cre-ER(T) negative (control) *Mapk14*^{fl/fl} mice.

Supplemental Figure 2. ELISA data showing time course of IL-6 secretion from murine cardiac fibroblasts stimulated with cardiac DAMPs. Blue filled circles represent DAMPs-stimulated IL-6 secretion and black filled squares represent basal secretion without addition of DAMPs (measured up to 6 h only). *$P<0.05$ compared with time zero (n=3).

Supplemental Table 1. Genotyping primer sequences and predicted PCR product sizes. See Fig.1A for binding positions of X, Y and Z primers and Fig. 1B for PCR gels.

Supplemental Table 2. Taqman primer/probes used for real-time RT-PCR. Purchased from Applied Biosystems.

Supplemental Table 3. Effect of fibroblast-specific p38α knockout on isoproterenol-induced microRNA expression - complete data set. See Fig. 4 legend for experimental details. A01-G12 = mean expression levels ($2^{-\Delta CT}$) of 84 cardiovascular microRNAs relative to normalisation controls. H01-H02 = negative controls; H03-H08 = normalisation controls; H09-H10 = reverse transcription positive controls; H11-H12 = PCR positive controls.
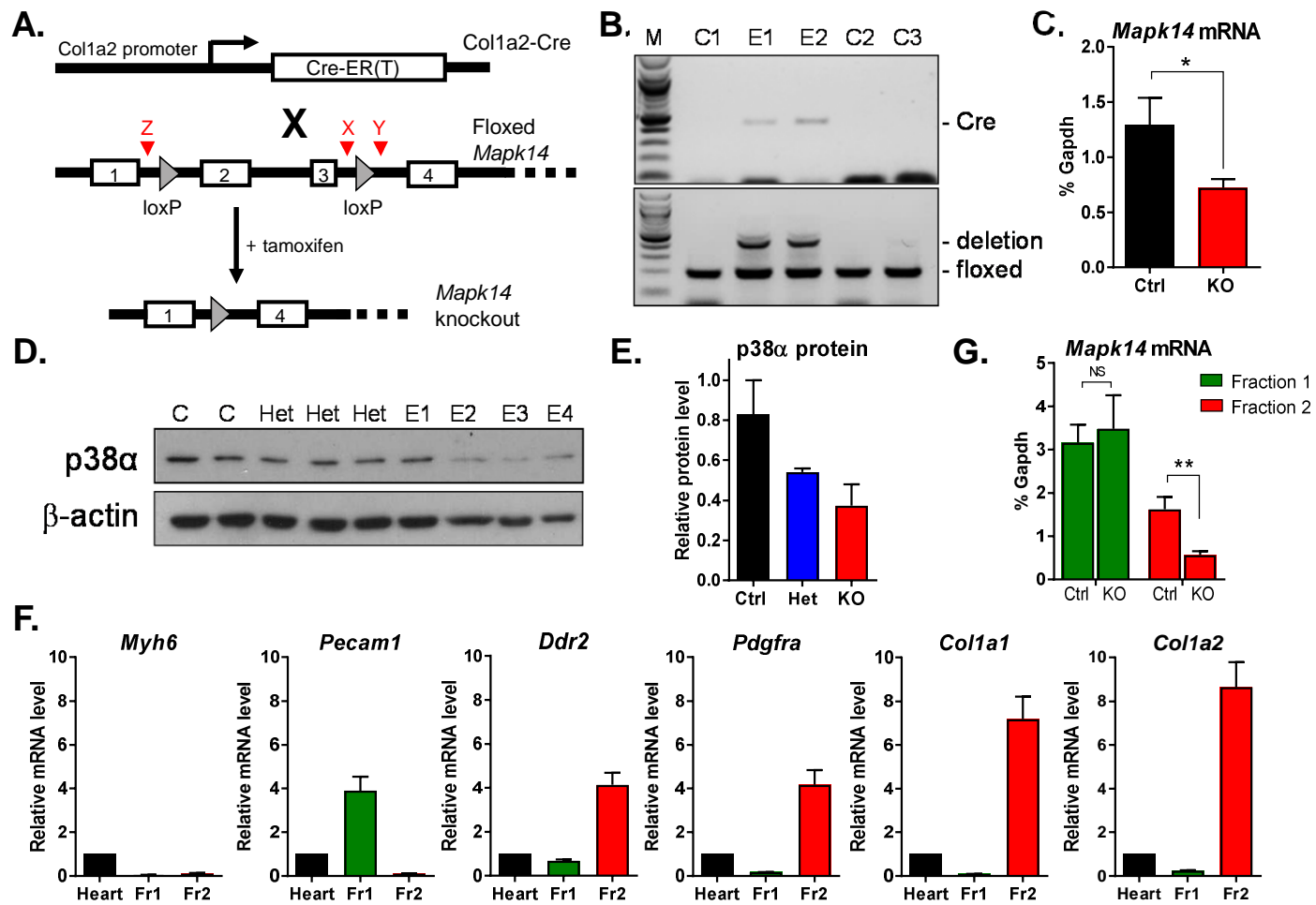
Figure 1
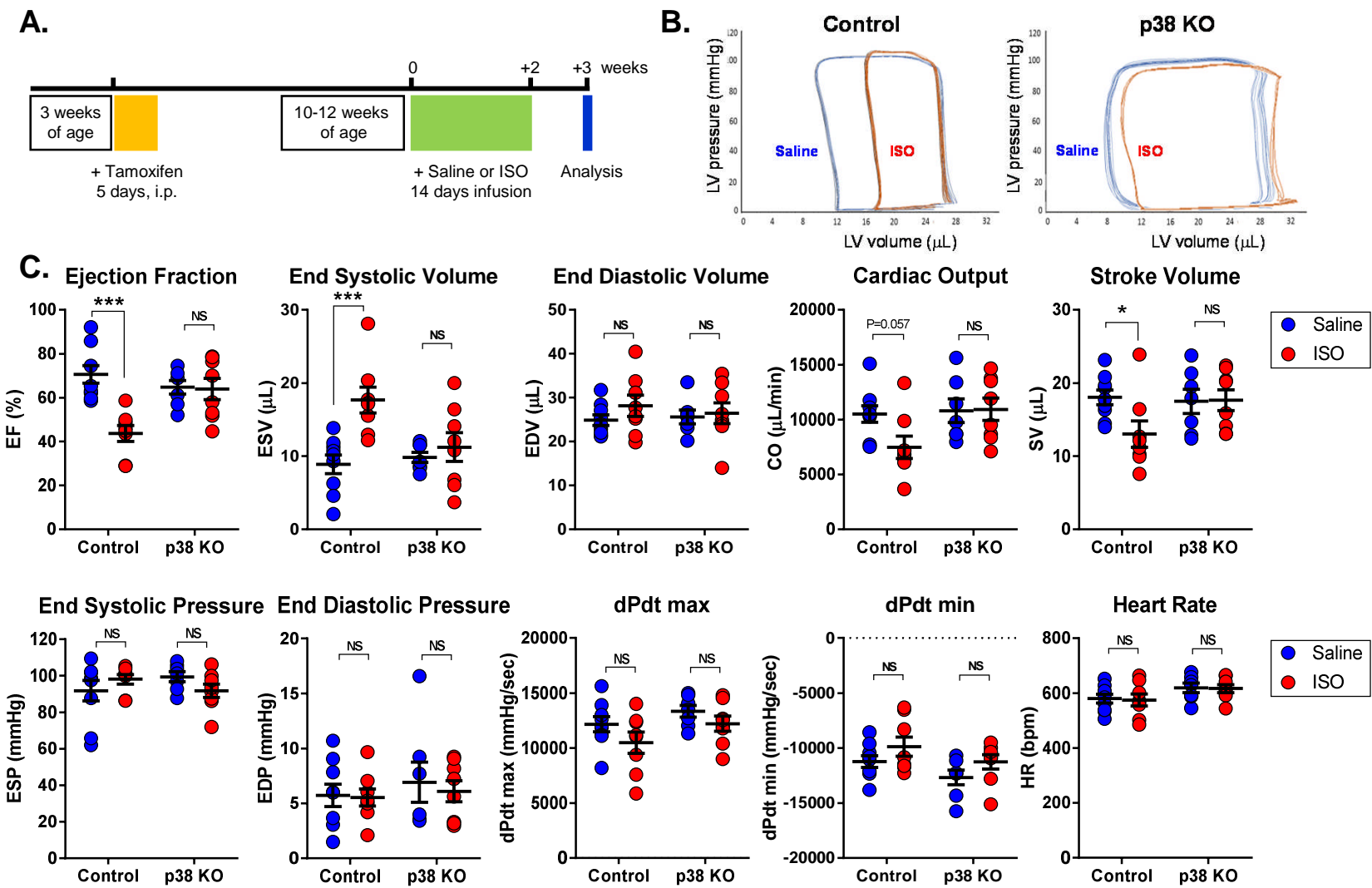
Figure 2

Figure 3

Figure 4

A.

ISO (min): 0 2 5 10 15 30

p-p38α

total p38α

DAMPs (min): 0 10 20 30

p-p38α

total p38α

ISO (μmol/L): 0 0.1 0.5 1 5 10

p-p38α

total p38α

B.

Fgf2 mRNA

Il6 mRNA

Tgfb1 mRNA

Igf1 mRNA

Figure 5

Figure 6

Col1a2Cre$^{+/-}$ *Mapk14*$^{fl/fl}$

Col1a2Cre$^{+/-}$*Mapk14*$^{fl/+}$ *Mapk14*$^{fl/fl}$
50%

Col1a2Cre$^{+/-}$*Mapk14*$^{fl/fl}$ *Mapk14*$^{fl/fl}$
50%

Col1a2Cre$^{+/-}$*Mapk14*$^{fl/fl}$ *Mapk14*$^{fl/fl}$
50%   50%

+ tamoxifen

Fibroblasts: p38α$^{-/-}$ p38α$^{fl/fl}$
Other cells: p38α$^{fl/fl}$ p38α$^{fl/fl}$
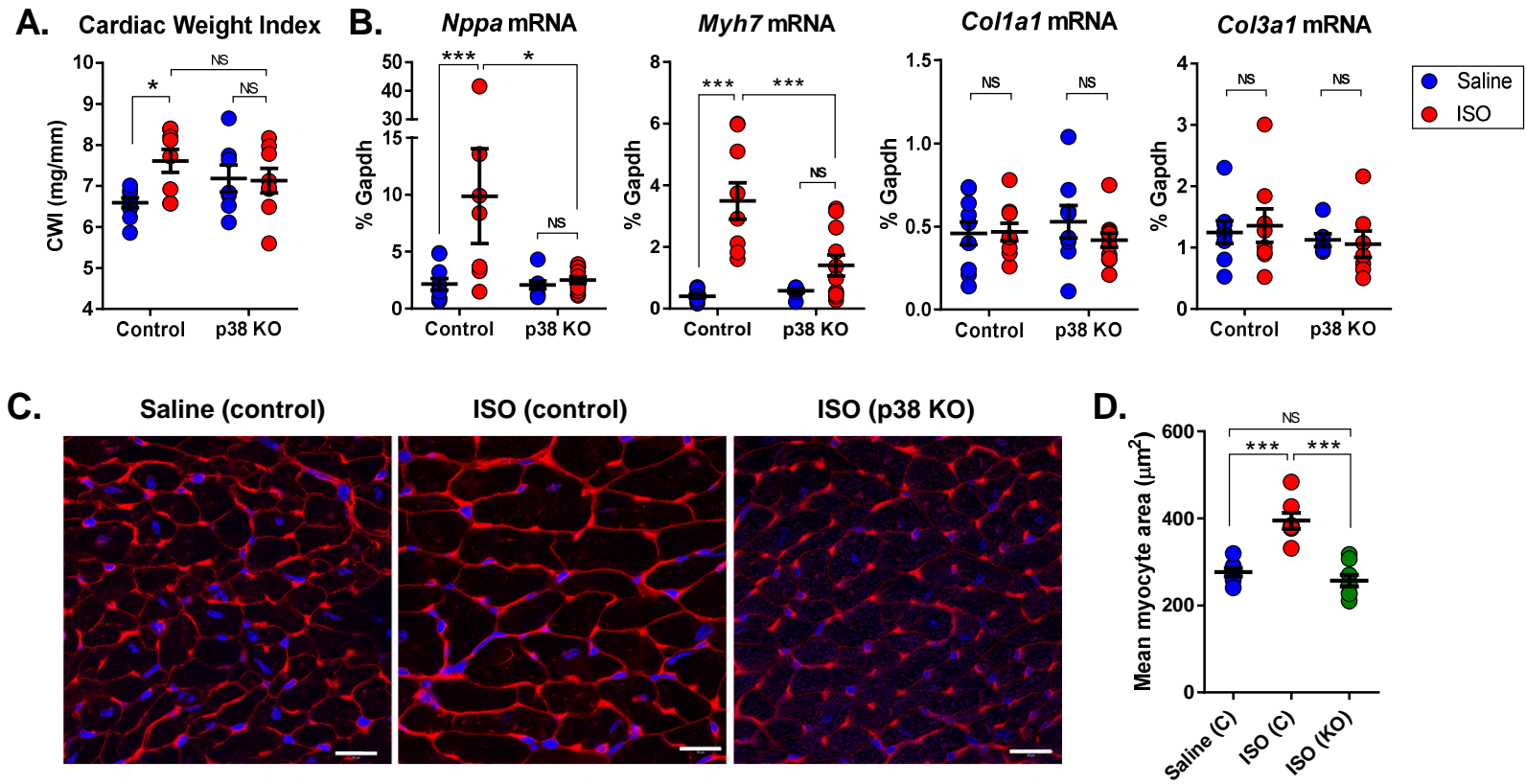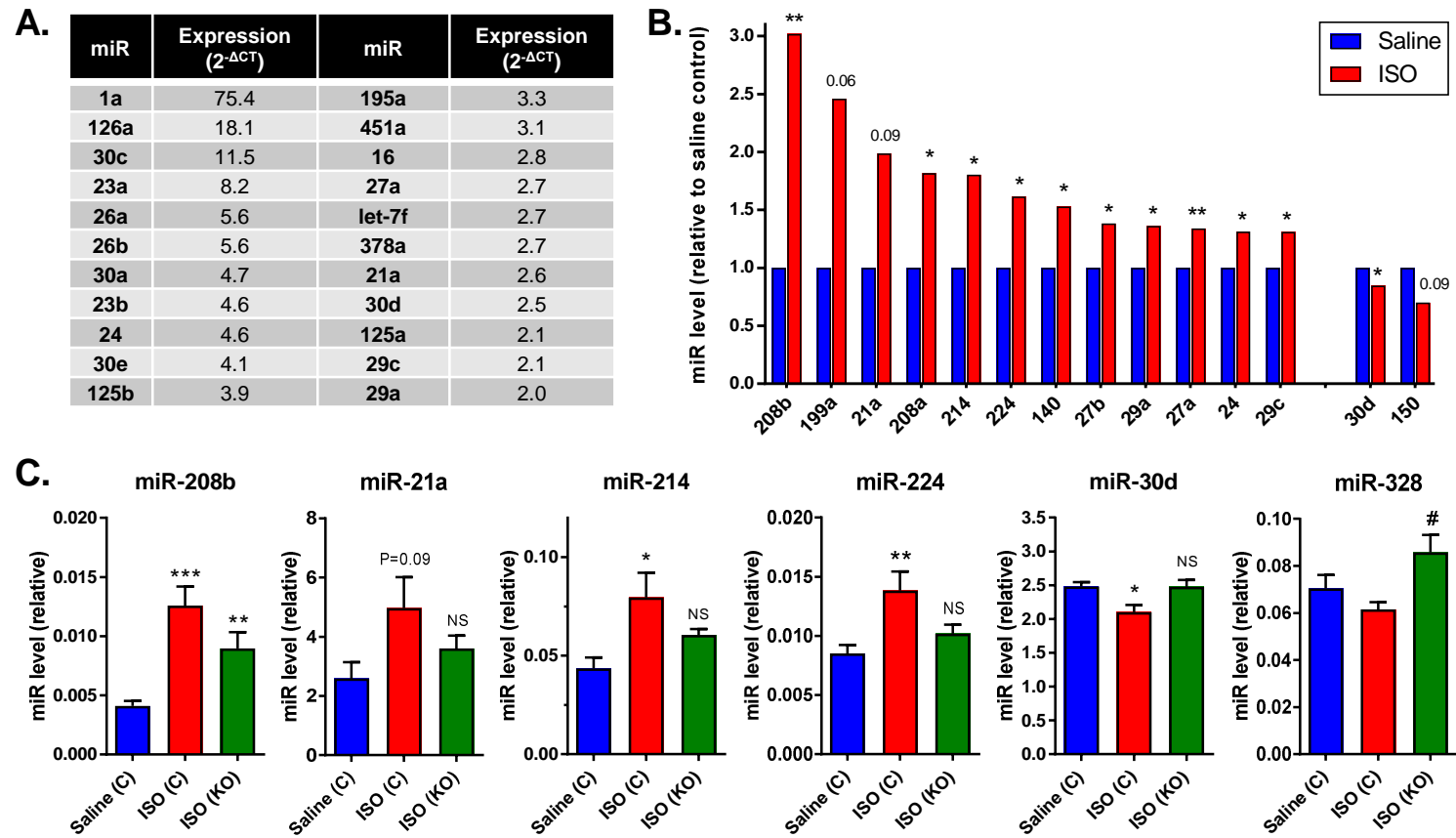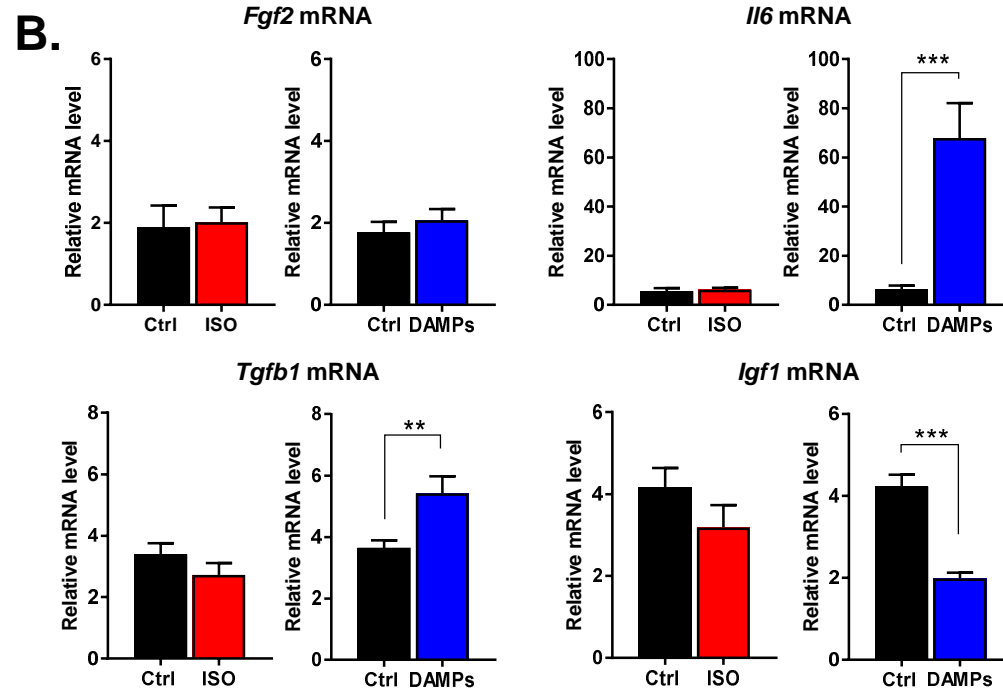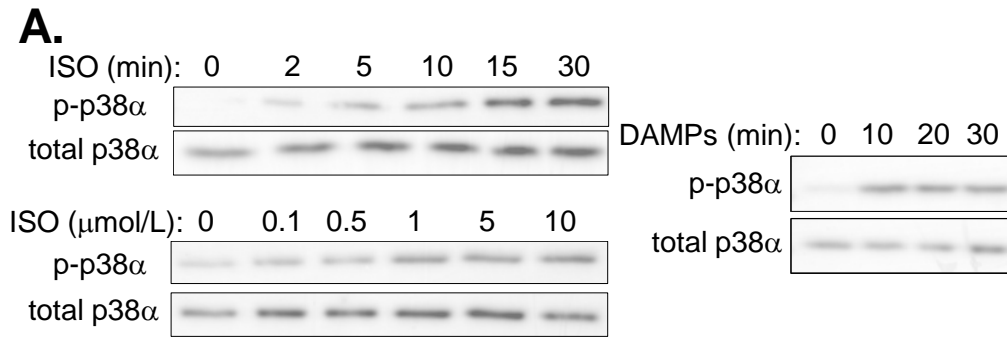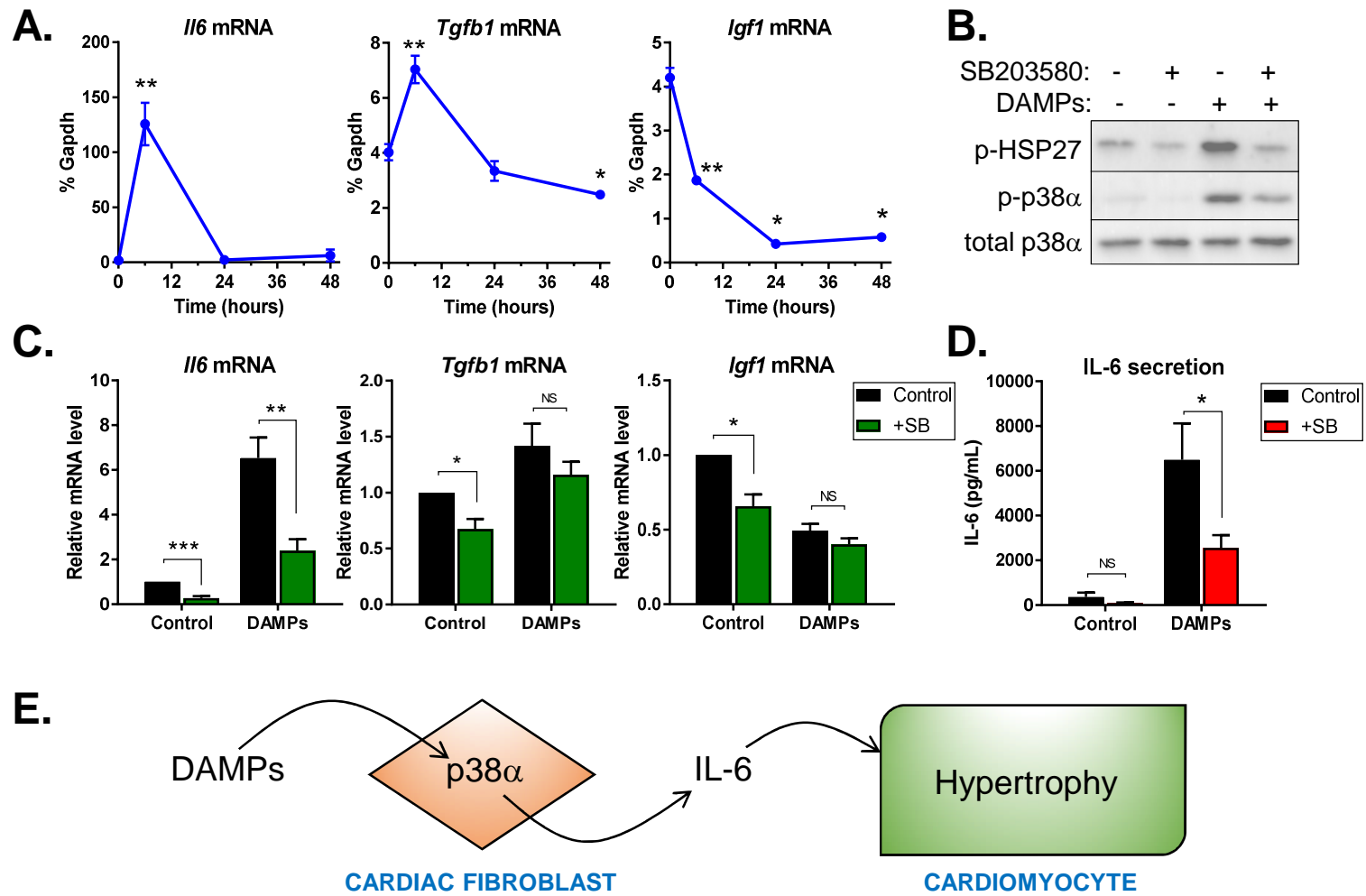
Supplemental Figure 1
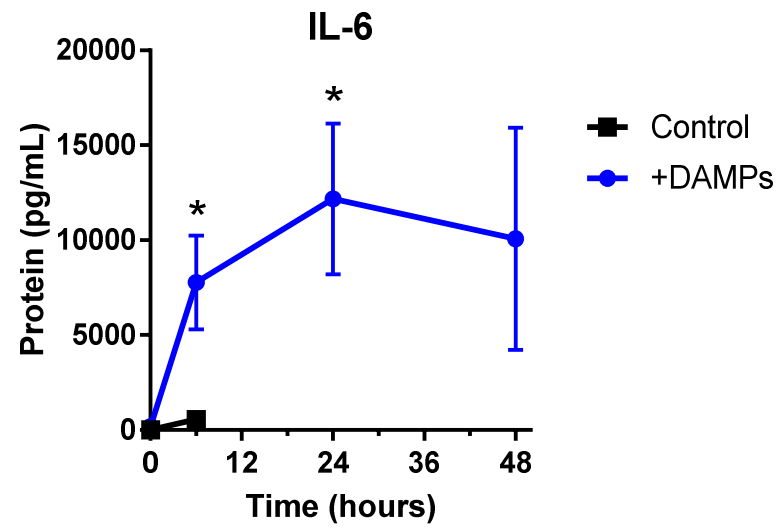
Supplemental Figure 2

Primer target	Primer sequence	Product size (bp)
Cre (forward) Cre (reverse)	5' GCATTACCGGTCGATGCAACGAGTGATGAG 3' 5' GAGTGAACGAACCTGGTCGAAATCAGTGCG 3'	408 (Cre)
p38 fl (forward) 'X' p38 fl (reverse) 'Y'	5' CTACAGAATGCACCTCGGATG 3' 5' AGAAGGCTGGATTTGCACAAG 3'	121 (wild type) 188 (floxed)
p38 del (forward) 'Z' p38 del (reverse) 'Y'	5' CCAGCACTTGGAAGGCTATTC 3' 5' AGAAGGCTGGATTTGCACAAG 3'	411 (deletion)

Supplemental Table 1

Gene	Protein	Code
Col1a1	Type 1 collagen α1 chain	Mm00801666_g1
Col1a2	Type 1 collagen α2 chain	Mm00483888_m1
Col3a1	Type 3 collagen α1 chain	Mm01254476_m1
Ddr2	Discoidin domain receptor 2	Mm00445615_m1
Fgf2	Fibroblast growth factor 2	Mm01285715_m1
Gapdh	Glyceraldehyde 3-phosphate dehydrogenase	Mm99999915_g1
Igf1	Insulin-like growth factor 1	Mm00439560_m1
Il6	Interleukin-6	Mm00446190_m1
Mapk14	p38α	Mm00442498_m1
Myh6	α-myosin heavy chain	Mm00440354_m1
Myh7	β-myosin heavy chain	Mm00600555_m1
Nppa	Atrial natriuretic factor	Mm01255747_g1
Pdgfra	Platelet-derived growth factor receptor A	Mm00440701_m1
Pecam1	Platelet and endothelial cell adhesion molecule 1 (CD31)	Mm01242584_m1
Tgfb1	Transforming growth factor-β1	Mm01178820_m1

Supplemental Table 2

		2^(-Avg.(Delta(Ct))		
Position	Mature ID	Control Saline	Control ISO	KO ISO
A01	mmu-let-7a-5p	1.978162	2.172275	2.041877
A02	mmu-let-7b-5p	0.605095	0.635914	0.668553
A03	mmu-let-7c-5p	1.532619	1.722121	1.680468
A04	mmu-let-7d-5p	1.093911	1.055471	1.085327
A05	mmu-let-7e-5p	0.645167	0.752254	0.711122
A06	mmu-let-7f-5p	2.549444	2.685828	2.68337
A07	mmu-miR-100-5p	0.161577	0.190837	0.195614
A08	mmu-miR-103-3p	0.168501	0.177769	0.20665
A09	mmu-miR-107-3p	0.019813	0.016775	0.021257
A10	mmu-miR-10b-5p	0.057463	0.066269	0.060276
A11	mmu-miR-122-5p	0.001465	0.001835	0.001801
A12	mmu-miR-124-3p	0.000606	0.00054	0.000723
B01	mmu-miR-125a-5p	2.114928	2.066103	2.071637
B02	mmu-miR-125b-5p	3.91234	4.221776	4.471839
B03	mmu-miR-126a-3p	17.952363	20.449608	22.115827
B04	mmu-miR-130a-3p	0.125548	0.142245	0.183198
B05	mmu-miR-133a-3p	0.246519	0.20525	0.346145
B06	mmu-miR-133b-3p	0.186687	0.170077	0.278785
B07	mmu-miR-140-5p	0.045359	0.069249	0.066466
B08	mmu-miR-142a-3p	0.142558	0.210599	0.30767
B09	mmu-miR-143-3p	1.263261	1.651269	2.050159
B10	mmu-miR-144-3p	0.001251	0.003234	0.008786
B11	mmu-miR-145a-5p	1.315416	1.537097	1.942239
B12	mmu-miR-146a-5p	0.167853	0.192358	0.158373
C01	mmu-miR-149-5p	0.265799	0.248161	0.288919
C02	mmu-miR-150-5p	1.324479	0.916346	1.188492
C03	mmu-miR-155-5p	0.107766	0.078496	0.102379
C04	mmu-miR-15b-5p	0.383261	0.527334	0.484747
C05	mmu-miR-16-5p	2.753326	3.155302	3.654376
C06	mmu-miR-17-5p	0.149944	0.173987	0.190662
C07	mmu-miR-181a-5p	0.058593	0.05478	0.076275
C08	mmu-miR-181b-5p	0.06097	0.054748	0.056639
C09	mmu-miR-182-5p	0.000525	0.000461	0.000501
C10	mmu-miR-183-5p	0.000413	0.000401	0.000279
C11	mmu-miR-185-5p	0.265257	0.216887	0.242893
C12	mmu-miR-18a-5p	0.00868	0.011482	0.013958
D01	mmu-miR-195a-5p	3.226149	3.795757	4.150002
D02	mmu-miR-199a-5p	0.01817	0.044725	0.042824
D03	mmu-miR-1a-3p	70.693992	57.04811	68.262464
D04	mmu-miR-206-3p	0.081044	0.062917	0.080414
D05	mmu-miR-208a-3p	0.016875	0.030677	0.072187
D06	mmu-miR-208b-3p	0.004045	0.012213	0.008761
D07	mmu-miR-21a-5p	2.354904	4.680181	3.506293
D08	mmu-miR-210-3p	0.008243	0.008814	0.010952
D09	mmu-miR-214-3p	0.04237	0.076406	0.060218
D10	mmu-miR-22-3p	0.445459	0.612899	0.83402
D11	mmu-miR-221-3p	0.0641	0.062163	0.075483
D12	mmu-miR-222-3p	0.083211	0.094821	0.095173

		2^(-Avg.(Delta(Ct))		
Position	Mature ID	Control Saline	Control ISO	KO ISO
E01	mmu-miR-223-3p	0.425817	0.472874	0.365973
E02	mmu-miR-224-5p	0.008408	0.013581	0.01008
E03	mmu-miR-23a-3p	7.999973	9.286721	9.355538
E04	mmu-miR-23b-3p	4.546558	5.77468	5.07496
E05	mmu-miR-24-3p	4.552592	5.973209	6.325244
E06	mmu-miR-25-3p	0.330425	0.356809	0.366763
E07	mmu-miR-26a-5p	5.55294	6.13263	5.966145
E08	mmu-miR-26b-5p	5.321684	5.695079	5.861896
E09	mmu-miR-27a-3p	2.688119	3.598146	3.907551
E10	mmu-miR-27b-3p	1.827181	2.527138	2.481245
E11	mmu-miR-29a-3p	2.030514	2.760202	3.347464
E12	mmu-miR-29b-3p	0.16203	0.17208	0.273372
F01	mmu-miR-29c-3p	2.071333	2.71383	3.550657
F02	mmu-miR-302a-3p	0.000156	0.000131	0.000148
F03	mmu-miR-302b-3p	0.000168	0.000136	0.000145
F04	mmu-miR-30a-5p	4.665472	4.58408	5.335247
F05	mmu-miR-30c-5p	11.472092	11.131246	11.736017
F06	mmu-miR-30d-5p	2.479405	2.091413	2.4688
F07	mmu-miR-30e-5p	4.069234	4.195758	5.148764
F08	mmu-miR-31-5p	0.069383	0.071437	0.073627
F09	mmu-miR-320-3p	0.091621	0.088029	0.104023
F10	mmu-miR-322-5p	0.778961	1.025937	0.967987
F11	mmu-miR-328-3p	0.069698	0.061058	0.084617
F12	mmu-miR-342-3p	0.116092	0.128755	0.120102
G01	mmu-miR-365-3p	0.144937	0.16812	0.159335
G02	mmu-miR-378a-3p	2.601141	2.371442	2.592555
G03	mmu-miR-423-3p	0.028334	0.024852	0.026223
G04	mmu-miR-451a	2.966517	3.46716	5.613137
G05	mmu-miR-486b-5p	0.413167	0.363977	0.426565
G06	mmu-miR-494-3p	0.00124	0.001414	0.001263
G07	mmu-miR-499-5p	0.646546	0.535546	0.626917
G08	mmu-miR-7a-5p	0.017609	0.018226	0.017562
G09	mmu-miR-92a-3p	0.304953	0.340335	0.337351
G10	mmu-miR-93-5p	0.077645	0.089542	0.118528
G11	mmu-miR-98-5p	0.05129	0.062569	0.051151
G12	mmu-miR-99a-5p	1.092071	1.304632	1.489604
H01	cel-miR-39-3p	0.000155	0.000127	0.000138
H02	cel-miR-39-3p	0.000155	0.000127	0.000138
H03	SNORD61	0.476724	0.528432	0.585235
H04	SNORD68	4.458221	4.156111	3.940604
H05	SNORD72	0.410206	0.443319	0.368542
H06	SNORD95	0.639813	0.605386	0.600758
H07	SNORD96A	2.354499	2.192101	2.094829
H08	RNU6-6P	0.650187	0.673129	0.816331
H09	miRTC	0.237416	0.226773	0.282779
H10	miRTC	0.236745	0.245652	0.305355
H11	PPC	6.19832	5.10393	5.24695
H12	PPC	6.160693	5.442311	5.218452

Supplemental Table 3